Electronic Supplementary Material (ESI) for Physical Chemistry Chemical Physics.

Electronic Supplementary Information

Energy dissipative photo-protective mechanism of carotenoid spheroidene from the photoreaction center of purple bacteria *Rhodobacter sphaeroides*

Sundaram Arulmozhiraja,[a] Naoki Nakatani,[a] Akira Nakayama,[a] and Jun-ya Hasegawa*[a, b]

[a] *Catalysis Research Center, Hokkaido University, Kita 21, Nishi 10, Kita-ku, Sapporo 001-0021, Japan*

[b] JST-CREST

S1. Detailed description of the research background

Reaction center (RC) of purple bacteria, *Rhodobacter (Rb.) sphaeroides*, Figure S1, consists of three subunits (H, L, and M) with cofactors including four bacteriochlorophylls (BChl), in which two of them formed as a special pair (SP) that is a primary electron donor, two bacteriopheophytins (BPhe), two ubiquinones (UQ), a nonheme iron, and a spheroidene (SPO) carotenoid (Figure S2). All these cofactors form into two symmetrical groups, normally denoted as L and M branches. Though the reaction center is structurally symmetric, it is functionally asymmetric – electron transfer happens only in the L branch!

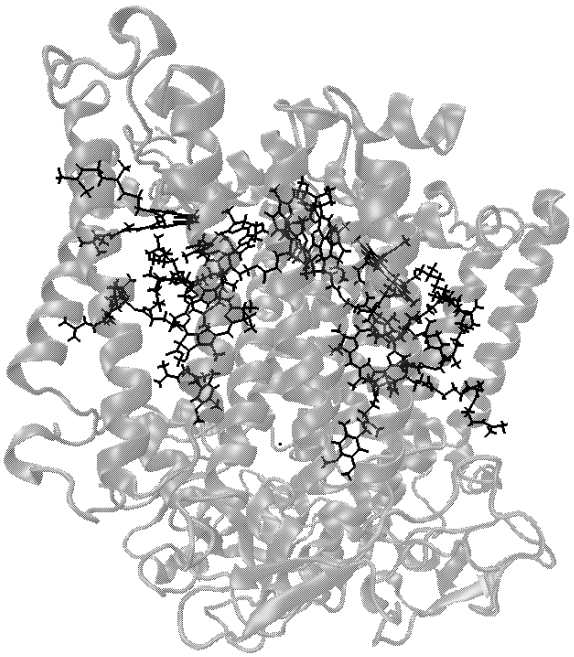

Figure S1. Schematic structure of the purple bacteria *Rhodobacter (Rb.) sphaeroides* (PDB id 2J8C).[1]

Upon absorbing light, the RC initiates electron transfer from its special pair through a series of electron acceptor cofactors to reduce its bound ubiquinone (UQ_M). Full reduction of the quinone requires transfer of two electrons and subsequently it takes up two protons from the solution and becomes quinol. Following reduction, the quinol released from the RC into the membrane and gets reoxidized by the cytochrome complex, releasing protons on the opposite side of the membrane. This action is coupled with cycling of the electrons back to the RC via a cytochrome. This light induced proton pump brings to a transmembrane proton gradient, which is utilized for ATP synthesis. Thus RC involves in vital transfer of electrons and transport of protons.

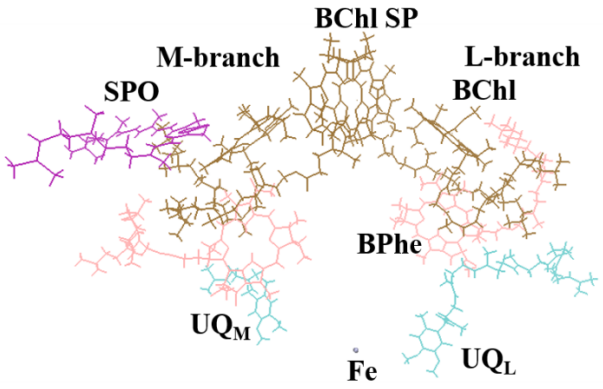

Figure S2. Reaction center of the purple bacteria *Rhodobacter (Rb.) sphaeroides* (PDB id 2J8C). {Koepke, 2007 #26}

Among the co-factors of RC, carotenoid plays a dual role: as a light-harvester (LH) in antenna complexes and as a photo-protector (PP) in bacterial reaction centers.[2-12] As a LH, carotenoid absorbs the blue-green light that is not absorbed by the bacteriochlorophyll cofactors and transfer its singlet state excitation energy to the special pair through the accessory BChl, whereas as a PP, it quenches triplet BChl special pair to prevent sensitized generation of singlet oxygen ($^1\Delta_g$).[13, 14] The latter quality of the carotenoids is utilized essentially by all the photosynthetic organisms. In fact the carotenoids are best known as efficient quenchers of not only the dangerous singlet oxygen but also of various reactive intermediate radicals by intercepting the chain of oxidative reactions. This antioxidative function of carotenoids is a key mechanism for the protection of many diseases including cancer and macular degeneration in humans.[15-17]

In RC of *Rb.* sphaeroides, carotenoid spheroidene plays the photoprotective quencher role – when excess of light energy is supplied to the RCs under reducing conditions, it gives rise to reverse electron transfer and charge recombination at the special pair of bacteriochlorophylls to generate the triplet state, which can result in the sensitized formation of harmful singlet oxygen.[3, 18, 19] The triplet state of donor (special pair) is, however, normally quenched by the carotenoid through energy transfer that produces a triplet carotenoid.[20-27] This might be one of the main reasons for why this carotenoid bounded in the photosynthetic reaction center is in van der Walls contact with the accessory bacteriochlorophyll on the inactive M side though it does not participate directly in the electron transfer process.

Like other carotenoids, spheroidene is derived from the same basic structure of 40 carbon atoms resulting from the polymerization of eight units of isoprene, and can be considered as a conjugated polyene chain. It has 10 (n=10) conjugated C=C double bonds. Interestingly, it is speculated that spheroidene selects its configuration depending on its major function: all-*trans* configuration in the antenna complexes and 15,15′-*cis* configuration (Figure S3) in the bacterial reaction centers.

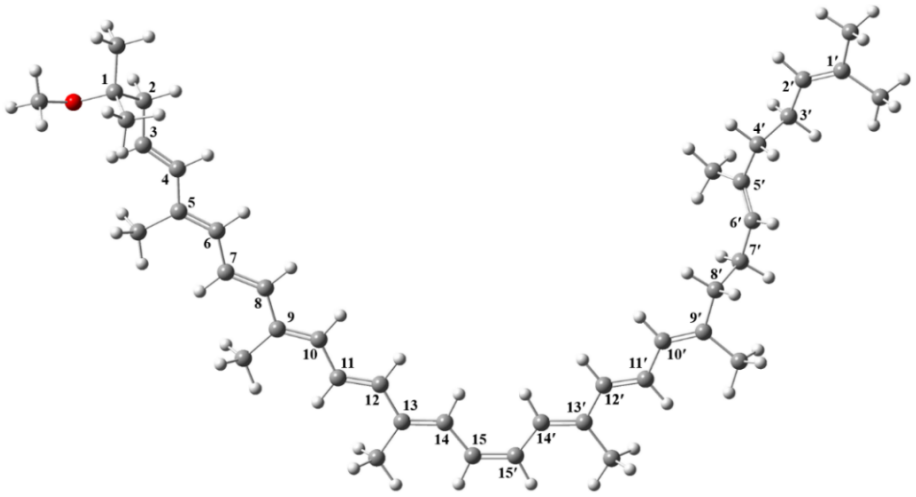

Figure S3. Structure (optimized) with important carbon atom numbering of 15,15′-*cis*-spheroidene.

There are number of possible stereoisomers for the carotenoids of pigment-protein complexes from photosynthetic organisms; however, the reason for the presence of a particular stereoisomer in these systems is not known convincingly. A big puzzle is that whether the natural selection of geometric isomers of carotenoids in these complexes is determined by the structure of the protein binding site or by the need for the organism to accomplish a particular biological task. The presence of carotenoids in their *cis* configurations in the reaction centers and *trans* configurations in the light-harvesting antenna complexes has led to the hypothesis that the stereoisomers play different roles.

Boucher and Gingras[28] showed isomerization of the RC-bound 15-*cis* spirilloxanthin into all-*trans* based on electronic absorption spectroscopy in the case of *Rhodospirillum rubrum* S1. Kuki et al.[29] revealed the 15-*cis* to all-*trans* isomerization of the same carotenoid spirilloxanthin in the light and the reverse isomerization in the dark for a reduced form of RC from *R. rubrum* S1. By using transient Raman, transient absorption spectroscopies and by HPLC analysis of triplet-sensitized isomerization, Koyama and co-workers[30-33] showed that 15,15′-*cis* isomer of spheroidene is extremely efficient in *cis*-to-*trans* isomerization in the T_1 state. From these studies, Koyama and co-workers postulated that the natural selection of the 15,15′-*cis* isomer of spheroidene in the reaction center enhances the ability of the carotenoid to dissipate triplet energy from SP via *cis*-to-*trans* isomerization in the protein.[29, 32] This hypothesis has been supported by transient Raman spectroscopy of photoexcited triplet states of various *cis*-isomers of β-carotene and spheroidene, which suggest more rapid dynamics for the isomerization of the 15,15′-*cis* carotenoid to its all-*trans* configuration compared to other

cis-isomers of the molecules. It has been argued that *cis*-to-*trans* isomerization of 15,15′-*cis* carotenoid is a mechanism that enhances photoprotection.[28, 29, 32, 33]

Later, Ohashi et al.[34] made a comparison of the ground state Raman spectrum of spheroidene in the reaction center of *Rb.* sphaeroides 2.4.1 with that free in *n*-hexane solution and suggested that the RC-bound spheroidene takes a 15,15′-*cis* configuration, which is twisted around the central C15-C15′ bond. The T_1 Raman spectrum indicated substantial twisting and in-plane distortion of the conjugated backbone. Based on these facts, a mechanism of triplet-energy dissipation by the RC-bound spheroidene, which involves an internal rotation around the central C15-C15′ bond, is proposed.[34]

However, a study by Bautista et al.[35] using the reaction centers of the carotenoidless mutant *Rb.* sphaeroides R-26.1 in which locked-15-15′-*cis*-spheroidene, which is incapable of undergoing *cis*-to-*trans* isomerization, was incorporated revealed that there is no difference in either the spectroscopic properties or the photochemistry compared to *Rb.* sphaeroides wild-type strain 2.4.1 reaction centers. The study concluded that the natural selection of the 15,15′-*cis* isomer of spheroidene for the incorporation into the reaction centers of *Rb.* sphaeroides is determined by the nature of the carotenoid binding pocket in the pigment-protein complex. Nevertheless, later studies by Koyama and co-workers[36, 37] supported their earlier assumption that the isomer geometry influences the manner in which the excited-state energy is dissipated (quenched) and *cis*-spheroidene conformer has an advantage over its *trans* counterpart in quenching the triplet energy. Their arguments are the following: (1) The quantum yield and the rate of *cis*-to-*trans* isomerization is maximum for the 15,15′-c*is* conformer in its triplet state and its rate of $T_1 \rightarrow S_0$ intersystem crossing is 6 times larger than that of the *trans* T_1 species; (2) Among the selected *cis* isomers, 15,15′-*cis* has the highest rate of sensitized *cis*-to-*trans* isomerization; (3) The rate of isomerization is on the same order of magnitude as the rate of intersystem crossing for 15,15′-*cis*. They argued that these results clearly indicate the advantage for the *cis* conformer in the triplet-energy dissipation and the rotational motion around the C15=C15′ bond initiates the $T_1 \rightarrow S_0$ relaxation. Therefore, the usage of the 15,15′-*cis* configuration is expected to be most advantageous in dissipating the triplet energy. Koyama and co-workers[36, 37] also updated their hypothetical mechanism of triplet-energy dissipation and concluded that this fast intersystem crossing should take place during the rotation before reaching the *trans* configuration or even within the 15,15′-*cis* T_1 potential minimum.

Yet, studies by Pendon et al.[38-40] in 2006 concluded against the hypothesis drawn by Koyama and co-workers. They reported ultrafast time-resolved spectroscopic studies of two pairs of stable geometric isomers of carotenoids including *trans*-spheroidene and 13,14-locked-*cis*-spheroidene, the latter of which is incapable of undergoing *cis*-to-*trans* isomerization. Their results reveal only a small difference in spectra, decay dynamics, and transfer times. With these results along with the fact that carotenoids occupy narrow binding pockets in semi-rigid environments in photosynthetic pigment-protein complexes,[41] which could prevent them to undergo configurational isomerization in site, they claim that there does not appear to be any built-in advantage in either triplet energy transfer or triplet decay afforded to *cis*- over *trans*-carotenoids owing simply to their distinct geometric isomeric forms. In parallel, in the same year, Koyama and co-workers[42] examined the T_1 state of the RC-bound 15,15′-*cis*-spheroidene using the time-resolved electron paramagnetic resonance spectroscopy at low temperatures, and their results support their earlier hypothetical mechanism of triplet-energy dissipation through rotational motions around the central double bonds. So the influence of the isomeric structure of the carotenoid spheroidene on the all-important triplet energy dissipation is quiet controversial. In other words, it is not known convincingly how the nature of the isomeric structure affects the excited-state properties, dynamics, and biological function of the carotenoids. Since spheroidene acts as photo-protectors by quenching the triplet bacteriochlorophyll special pair in reaction centers, the influence of its structural configuration on its triplet excited state dynamics is worth to be understood without any ambiguity.

One more fact is that though it is broadly accepted that spheroidene in the *Rb.* sphaeroides photosynthetic reaction center exists in the 15,15′-*cis* configuration, possibility of the existence of other conformer is not completely ruled out especially for the spheroidene reconstituted in the carotenoidless mutant *Rb*. sphaeroides RC. A recent combined resonance Raman spectroscopy and density functional theory (DFT) calculations on the resonance Raman spectra of spheroidene reconstituted into the reaction center of *Rb.* Sphaeroides R26 by Wirtz et al.[43] concluded that the carotenoid in the RC occurs in two configurations: 15,15′-*cis* and 13,14-*cis* isomers. Again by using the same methodology, Mathies et al.[44] compared the resonance Raman spectra of spheroidene in the wild-type RC of *Rb.* sphaeroides and reconstituted into the RC of *Rb.* sphaeroides mutant R26. They concluded that wild-type reaction center of *Rb.* sphaeroides contain only 15,15′-*cis* conformer of spheroidene while the reconstituted R26 reaction center of the same bacterium contains spheroidene in both 15,15′-

cis and 13,14-*cis* configurations. A combined resonance Raman spectra and DFT calculations on different configurations of spheroidene, including 15,15-*cis*, by Boereboom et al.[45] concluded that besides the most likely 15,15′-*cis* structure, 13,14-*cis* isomer remains a candidate for an additional spheroidene structure in the RC. If such an existence of a dual configuration of spheroidene in RC turns out to be more general, then it might create a lot of biological importance. So in this scenario, it is important to study the triplet state and triplet energy dissipation mechanism of this new conformer.

Foregoing facts disclose the need for a complete investigation on the triplet-energy dissipation mechanism of spheroidene in the reaction centers. Moreover, furthering the knowledge of triplet excited-state dynamics of this carotenoid can not only solve this divisive issue on whether natural selection of stereoisomers has physiological significance or not but it also can resolve a knot in the most important yet highly complicated photosynthetic reaction center science. Hence we decide to investigate the triplet-energy dissipative mechanism of spheroidene by using theoretical calculations. To the best of our knowledge, most of theoretical studies concerned spectroscopy and quenching mechanism in singlet excited states. [46-56] Although only a few of them[49, 51] showed the results of adiabatic triplet excitation energy of carotenoid compounds, there is no report on the potential energy surfaces for the triplet-state quenching in carotenoid.

In the present study both 15,15′-*cis*- and *trans*-spheroidene stereoisomers and their truncated models, containing only the conjugated central parts, are considered for the investigation. The main aim of the present study is to understand the all-important quenching mechanism of the carotenoid spheroidene, i.e., the $T_1 \rightarrow S_0$ relaxation mechanism. As detailed above, sensitized isomerization is a possible mechanism for this carotenoid to dissipate its triplet energy and hence we gave particular importance in studying the potential energy surface along the rotation around the central C-C double bond. The structure of the 15,15′-*cis*-spheroidene is taken from the X-ray structure (1.87 Å resolution) of the photosynthetic reaction center from *Rb.* Sphaeroides (PDB id 2J8C).[1] Also, since solving the existing controversy over the postulated mechanism by Koyoma and co-workers is essential, two other forms of the spheroidene, 13,14-*cis*- and locked-13,14-*cis*-spheroidene, were also considered for the present study.

S2. Singlet-triplet crossing of the mini-model (octa-2,4,6-triene).

The potential energy curves of both singlet and triplet states at the triplet optimized structures along the C15=C15′ bond rotation is studied to explore the possible singlet-triplet crossing. Complete rotational energy landscape is obtained for the 15,15′-*cis*-spheroidene by calculating its energies at ϕ(14,15,15′,14′)=0° to ϕ(14,15,15′,14′)=180° by steps of 10°, i.e., along the complete isomerization from *cis* to *trans* structure. At each fixed rotational bond angle (say ϕ, for the simplicity), all the remaining geometrical parameters (of triplet state) were optimized fully. In addition to these points, energies were also obtained at some extra points to get smooth potential energy curves.

For a reliability test, we considered a miniaturised spheroidene model (octa-2,4,6-triene), Figure S4, and studied its potential energies along the central C=C bond twisting using a similar methodology described above. For this benchmarking study, we used number of density functionals and *ab initio* theories. Triplet state structures at each points were optimized at respective level of theories except for CCSD(T) calculations, for which the MP2/cc-pVDZ optimized structures were used. By comparing the results obtained using different functionals with those of the high-level *ab initio* calculations, the most suitable density functional, for this particular purpose, can be identified and consequently that could be used for the main study.

The derived potential energy curves are depicted in Figure S5, which show singlet-triplet crossing. As is seen in the Figure S5, the triplet energy surface is very flat all along the rotation – the change in energy from *cis* conformer to the *trans* is only around 1-2 kcal/mol. All the density functionals corroborate very well with the high-level *ab initio* CCSD(T) theory in producing the triplet energy surface. This is however not completely true for the singlet state case: though all the selected functionals could produce a similar trend as that of the CCSD(T) level, there is a significant difference in energy barrier as well as in angle at which singlet-triplet crossing ($\phi_{S\text{-}T}$) occurs. Nonetheless, the main concern here is the singlet-triplet crossing point rather than finding out the exact energy barrier. So let us keep aside the energy barrier difference and analyse the former.

The calculated crossing point varies from 50° to 80° with the different functional used. Various density functionals, B3LYP, BLYP,[57, 58] BP86,[57, 59] B3LYP*,[60] M06-2X,[61] M11,[62] and B2PLYPD (ref[63]), were checked against the second-order Moller-Plesset (MP2) level of

theory,[64, 65] the coupled-cluster singles and doubles with truncated triples [CCSD(T)],[66-68] and Brueckner doubles with truncated triples [BD(T)], ref[69-71], theories. For all the DFT calculations, 6-311G(*d*) basis set was used and for the *ab initio* calculations, Dunning's correlation-consistent double-zeta cc-pVDZ basis set was utilized.[72] In the result, both pure functionals (BP86 and BLYP) produce results that are very close to the CCSD(T) result: singlet-triplet crossing occurs at around $\phi_{S\text{-}T}$ = 75°. In fact, the singlet energy rotational barriers obtained using these two pure functionals have the least difference with that using the CCSD(T) theory. The other facts worth to be noticed here are that Hartree-Fock (HF) method significantly underestimates the singlet-triplet energy gap and MP2 theory overestimates the same, which reflect the well-known shortcoming of these theories. In fact it is not only the singlet-triplet energy gap overestimation issue, but the $\phi_{S\text{-}T}$ angle obtained using the MP2 is almost 10° higher than that obtained with CCSD(T). We also checked the MP2 results with a larger basis set, cc-pVTZ, to minimize the errors caused by the incompleteness of the basis set. But the results are the same, see Figure S6. Next to the pure functionals, two other functionals that provide better results are the double-hybrid B2PLYPD functional and the B3LYP* (B3LYP but with a reduced Hartree-Fock exchange amount) functional.

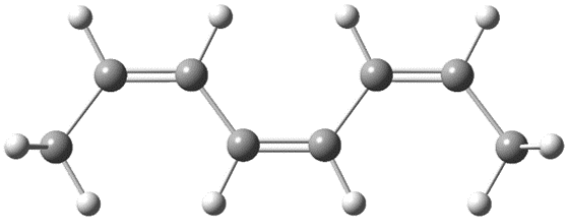

Figure S4. Mini-model of 15,15′-*cis* spheroidene.

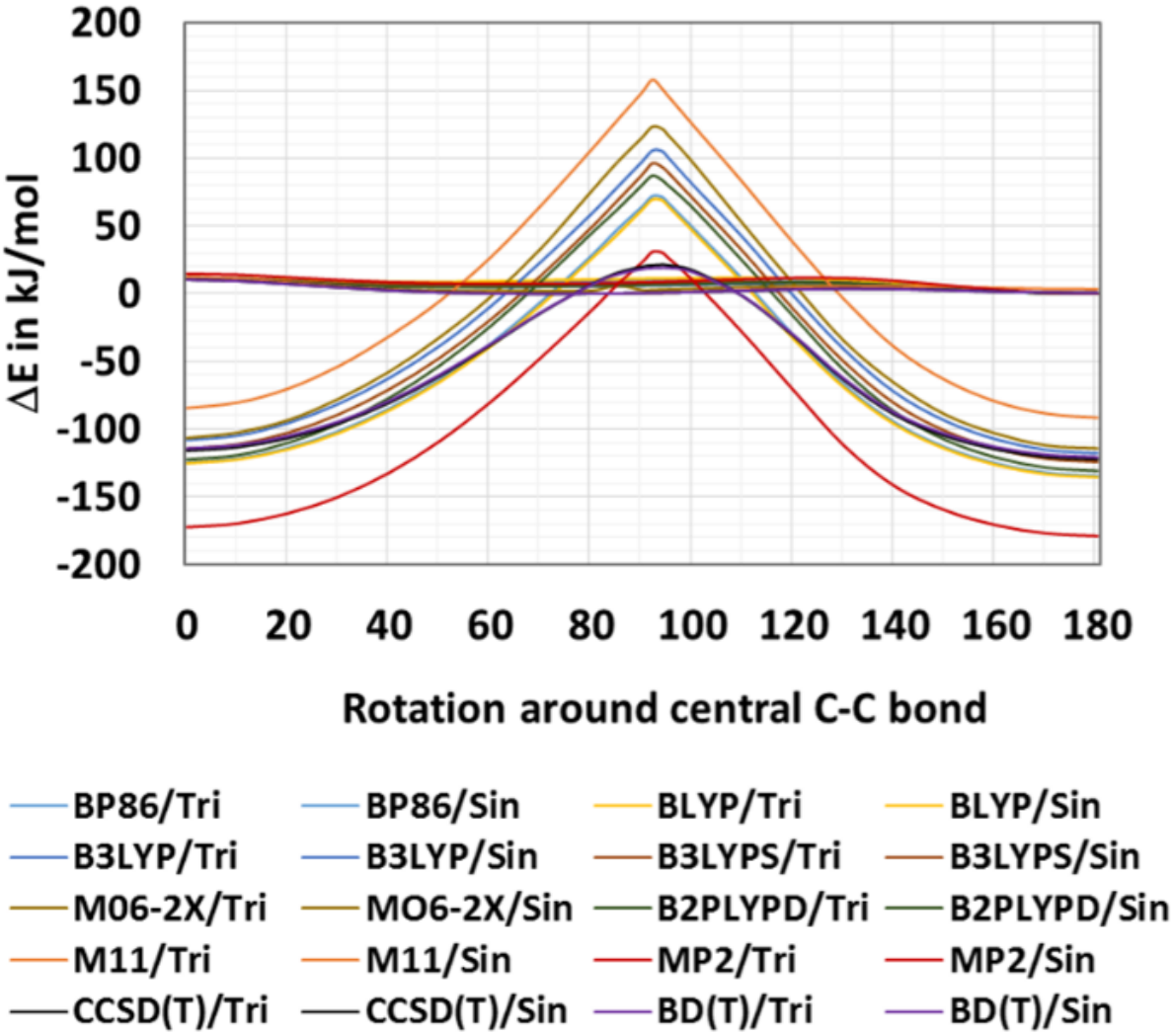

Figure S5. Singlet-triplet crossing of the mini-model of 15,15′-*cis* spheroidene. "Theory/Tri" represents the triplet energies obtained at their respective optimized structures and "Theory/Sin" represents singlet energies obtained at the respective triplet optimized structures. (See computational details for further details).

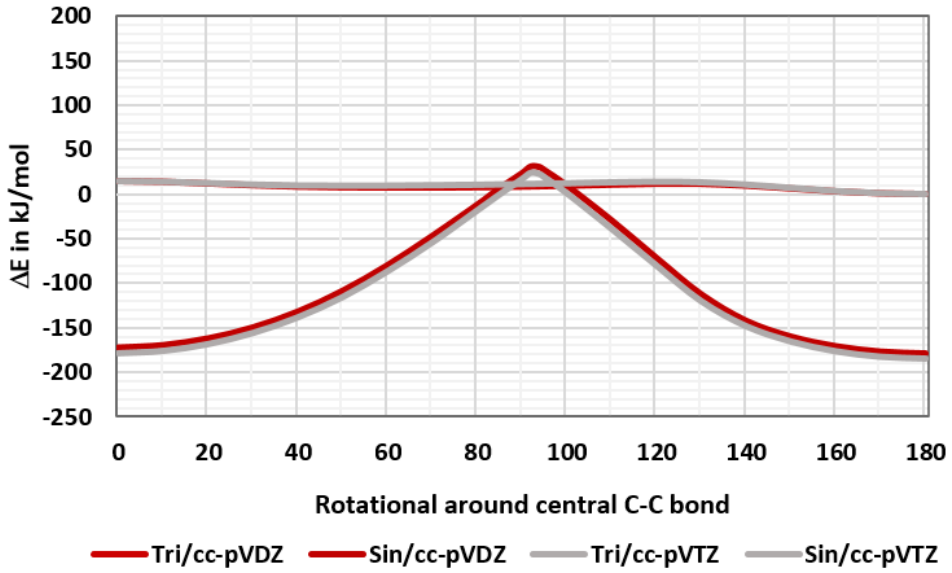

Figure S6. Singlet-triplet crossing of the mini-model.

Spin contamination might be an issue with the UCCSD(T) theory calculation for the triplet state especially when the UHF reference is poor. To check the reliability of the DFT results further, we studied the singlet-triplet crossing of this miniaturized spheroidene model by using BD(T) level of theory that eliminates the problematic singles amplitudes.[73-75] As in the case of CCSD(T) calculations, MP2/cc-pVDZ triplet state structures, optimized at every points, were used for the BD(T) study and the results are given in Figure S5. As the figure reveals, there is no difference in results obtained using CCSD(T) and BD(T) theories as the CCSD(T) $<S^2>$ values are within the allowed error bar (the obtained $<S^2>$ values are around 2.3). All these results clearly support the fact that reliable potential energy curves, especially singlet-triplet crossing, can be obtained using the BP86 and BLYP pure density functionals with 6-311G(*d*) basis set. So in the present investigation we use BP86 functional for all the remaining potential energy studies. One other point worth to be noted here is that the calculated energy difference between the *cis* and *trans* form of this mini model in their ground states is 1.92 and 1.93 kcal/mol at CCSD/cc-pVDZ and BD/cc-pVDZ level of theories, respectively. The same value derived using BP86 and B3LYP functional, with 6-311G(*d*) basis set, is 2.17 and 2.18 kcal/mol, respectively. These calculated values strongly support the reliability of the *cis-trans* energy differences reported for the truncated spheroidene pigment in the previous section.

S3. Convergence behaviour of the MEISC point searches

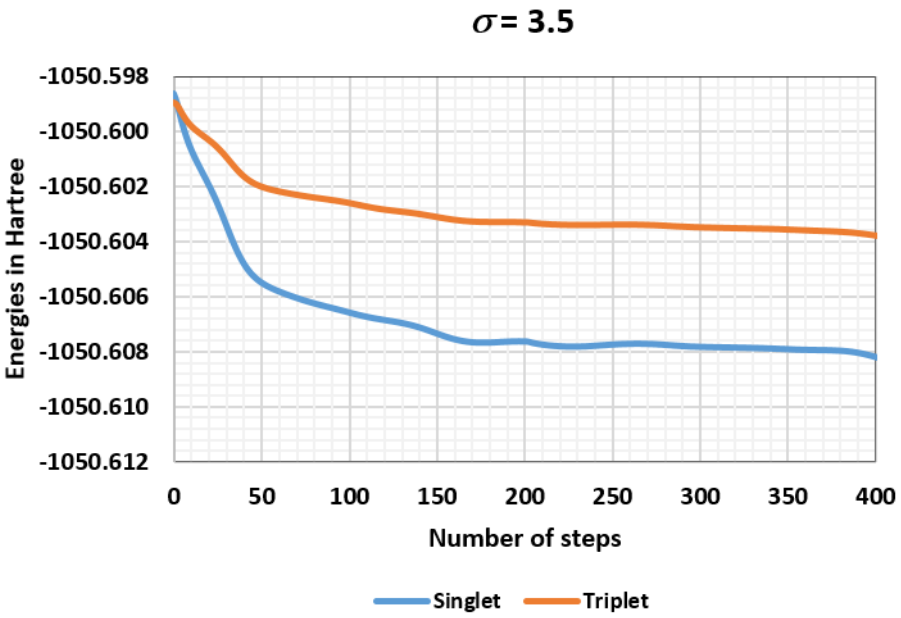

Figure S7. Convergence behaviour of singlet-triplet energy gap during MECI optimization with $\sigma = 3.5$.

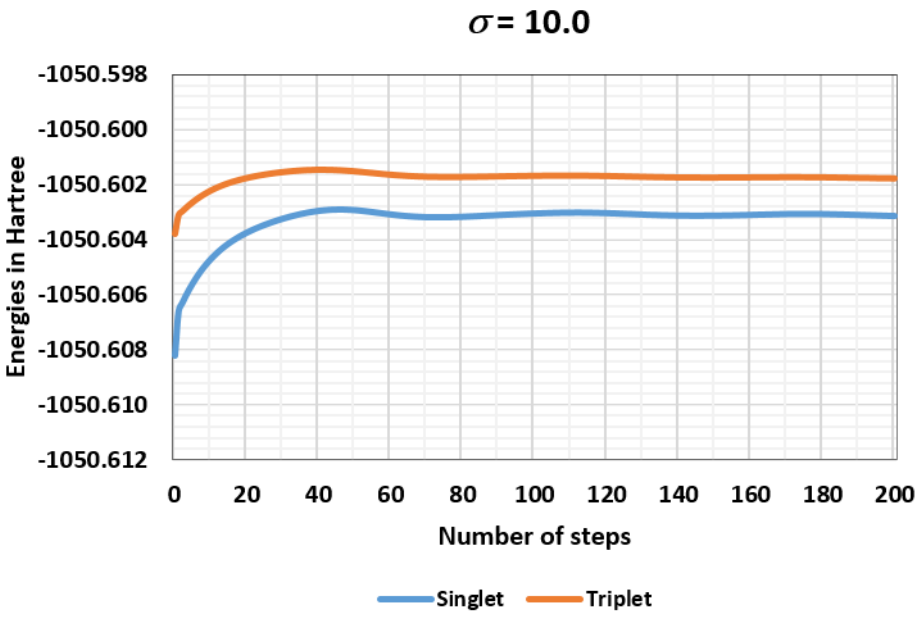

Figure S8. Convergence behaviour of singlet-triplet energy gap during MECI optimization with $\sigma = 10$.

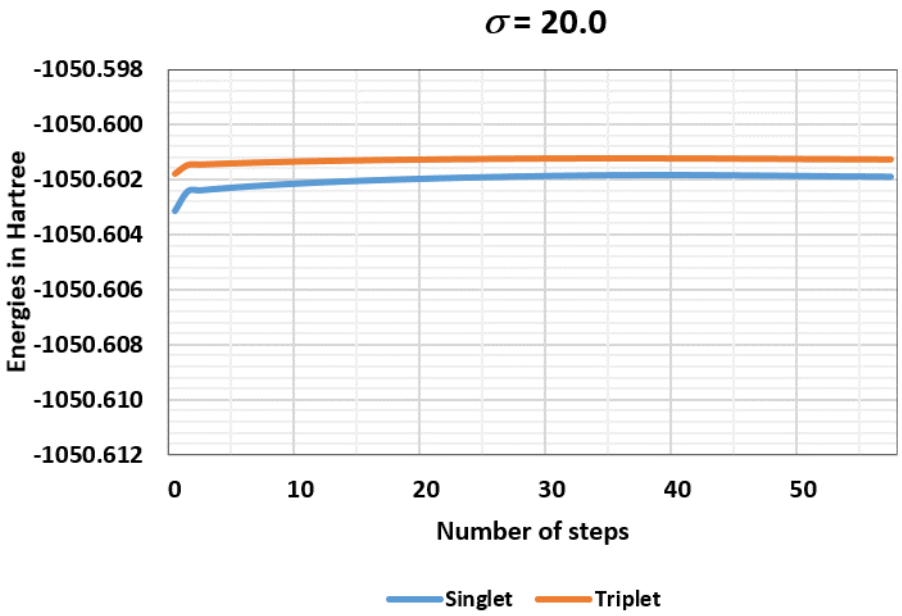

Figure S9. Convergence behaviour of singlet-triplet energy gap during MECI optimization with $\sigma = 20$.

S4. Potential energy curves for the C15-C15' rotation in solution

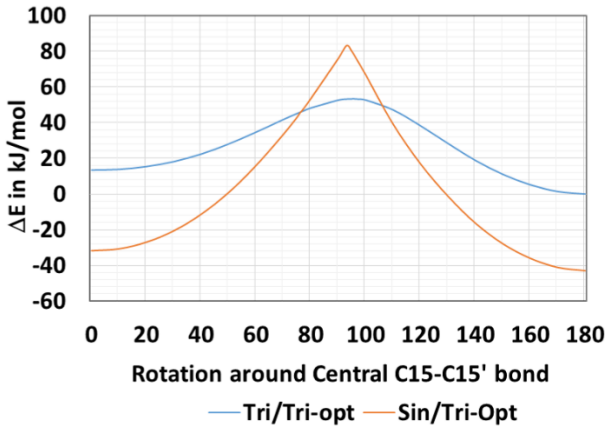

Figure S10. Singlet-triplet crossing of the 15,15′-*cis* spheroidene in *n*-hexane. Tri/Tri-Opt represents the triplet energies obtained at their respective optimized structures and Sin/Tri-Opt represents singlet energies obtained at the triplet optimized structures.

S5. Optimized structures

BP86/6-311G(*d*) optimized structure at the singlet-triplet crossing point [at ϕ(14,15,15′,14′) = 77°]

C1	-3.024058	-2.553287	0.264935
C2	-4.285474	-2.033074	0.808631
C3	-5.043004	-1.052966	0.219274
C4	-6.324917	-0.578662	0.662445
C5	-6.937560	-1.176713	1.904786
C6	-6.964163	0.421313	-0.091507
C7	-8.207852	1.018710	0.137243
C8	-8.751187	2.027482	-0.709046
C9	-9.955997	2.681078	-0.583015
C10	-10.94465	2.426217	0.523349
C11	-10.36993	3.727745	-1.583088
C12	-1.823034	-1.907827	0.337162
C13	-0.542988	-2.414943	-0.109519
C14	-0.486819	-3.786153	-0.737378
C15	0.578708	-1.616894	0.068428
C16	1.926059	-1.899529	-0.280914
C17	2.973402	-1.016030	-0.041639
C18	4.341377	-1.213676	-0.361462
C19	4.770638	-2.496783	-1.036024
C20	5.259874	-0.191510	-0.037220
C21	6.637711	-0.158507	-0.262912
C22	7.451612	0.935027	0.119996
C23	8.823593	1.091958	-0.048836
C24	9.693203	0.053730	-0.714354
C25	9.441961	2.306375	0.437337
C26	10.76057	2.634582	0.366129
C27	11.34818	3.910632	0.889325
H28	-4.721220	-2.609410	1.638434
H29	-4.630451	-0.571362	-0.678093
H30	-6.257454	-1.081375	2.769167
H31	-7.134028	-2.256186	1.773881
H32	-7.888646	-0.702274	2.180549
H33	-6.413660	0.775404	-0.975680
H34	-8.795179	0.698164	1.004234
H35	-8.125766	2.313100	-1.567541
H36	-10.61354	1.665264	1.243220
H37	-11.91810	2.097473	0.113377
H38	-11.15042	3.354429	1.088707
H39	-10.54372	4.705660	-1.094463
H40	-11.32568	3.460886	-2.073546
H41	-9.615797	3.874150	-2.371479
H42	-3.041028	-3.603479	-0.064004
H43	-1.818188	-0.896842	0.767312
H44	-0.841813	-4.560291	-0.033984
H45	-1.139758	-3.842681	-1.625894
H46	0.526166	-4.069664	-1.052298
H47	0.406114	-0.638862	0.540868
H48	2.152593	-2.857423	-0.761589
H49	2.720076	-0.062777	0.444115

H50	4.485648	-3.377933	-0.435642
H51	4.287669	-2.610847	-2.022297
H52	5.855633	-2.549298	-1.195273
H53	4.829935	0.692413	0.456296
H54	7.111883	-1.013190	-0.756644
H55	6.928937	1.765711	0.616565
H56	9.124747	-0.817838	-1.064556
H57	10.21910	0.478139	-1.587656
H58	10.47266	-0.314605	-0.023984
H59	8.762415	3.029204	0.912453
H60	11.46502	1.934521	-0.101173
H61	10.58322	4.558600	1.345912
H62	12.12604	3.716287	1.651009
H63	11.84508	4.487153	0.086923

MECI structure at BP86/6-311G(*d*) level

C1	-3.029528	-2.725752	0.379817
C2	-4.349557	-2.236442	0.824601
C3	-5.006345	-1.170861	0.284149
C4	-6.303290	-0.665824	0.689059
C5	-7.016067	-1.337218	1.836374
C6	-6.847612	0.415301	-0.009528
C7	-8.102843	1.024855	0.174314
C8	-8.563680	2.104845	-0.623651
C9	-9.781832	2.750935	-0.557722
C10	-10.87248	2.399636	0.419108
C11	-10.10592	3.875072	-1.505670
C12	-1.891089	-1.988251	0.363755
C13	-0.573719	-2.447114	-0.076918
C14	-0.446813	-3.867085	-0.570969
C15	0.486224	-1.571256	-0.013755
C16	1.856820	-1.823019	-0.358623
C17	2.868501	-0.902006	-0.187365
C18	4.259211	-1.103943	-0.474570
C19	4.699836	-2.424786	-1.061361
C20	5.161191	-0.073172	-0.181434
C21	6.558872	-0.066493	-0.349547
C22	7.372658	1.019467	0.026111
C23	8.762753	1.134768	-0.075351
C24	9.632544	0.046740	-0.656219
C25	9.388624	2.344523	0.400940
C26	10.72143	2.631414	0.391635
C27	11.31997	3.906619	0.903830
H28	-4.828650	-2.811802	1.629594
H29	-4.519805	-0.645326	-0.549334
H30	-6.351497	-1.428172	2.713119
H31	-7.333233	-2.362173	1.571532

H32	-7.910185	-0.787410	2.159514
H33	-6.225481	0.828338	-0.817333
H34	-8.765673	0.635508	0.954233
H35	-7.862962	2.460691	-1.393307
H36	-10.58385	1.622595	1.140317
H37	-11.77611	2.042934	-0.110811
H38	-11.18818	3.289564	0.994581
H39	-10.33151	4.811263	-0.960027
H40	-11.00875	3.648788	-2.104926
H41	-9.281240	4.082479	-2.204721
H42	-2.989815	-3.779128	0.066761
H43	-1.948299	-0.949671	0.717348
H44	-0.669041	-4.590197	0.233860
H45	-1.167820	-4.066245	-1.383029
H46	0.555241	-4.097823	-0.955420
H47	0.269754	-0.562293	0.366130
H48	2.114771	-2.810589	-0.755825
H49	2.595992	0.080554	0.223922
H50	4.456914	-3.263196	-0.385089
H51	4.185576	-2.626110	-2.017151
H52	5.779438	-2.464664	-1.255925
H53	4.723745	0.839777	0.248398
H54	7.037514	-0.951887	-0.780423
H55	6.849923	1.882702	0.463558
H56	9.055535	-0.819002	-1.006733
H57	10.21714	0.422595	-1.514217
H58	10.36162	-0.320877	0.087465
H59	8.708287	3.103444	0.814625
H60	11.42711	1.894602	-0.012893
H61	10.55251	4.593534	1.294531
H62	12.04791	3.715978	1.714257
H63	11.87903	4.438779	0.111772

S6. Singlet-triplet crossing of the full 15,15'-cis-spheroidene along C15-C15' bond rotation

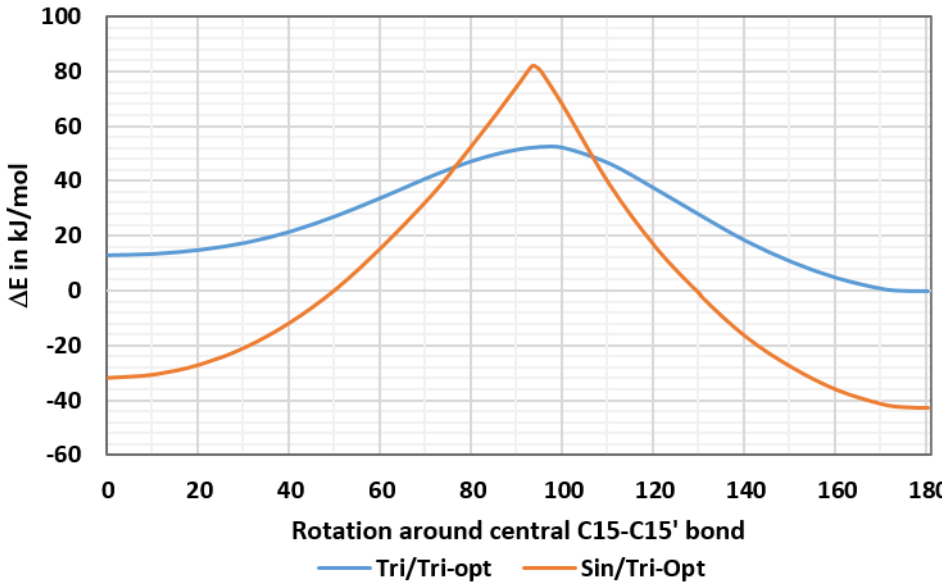

Figure S11. Singlet-triplet crossing of the full 15,15′-*cis*-spheroidene along C15-C15′ bond rotation.

S7. Variation in singlet state energy along C13-C14 (in 13,14-*cis*-) and C15-C15' (in 15,15'-cis-spheroidene) bond rotations

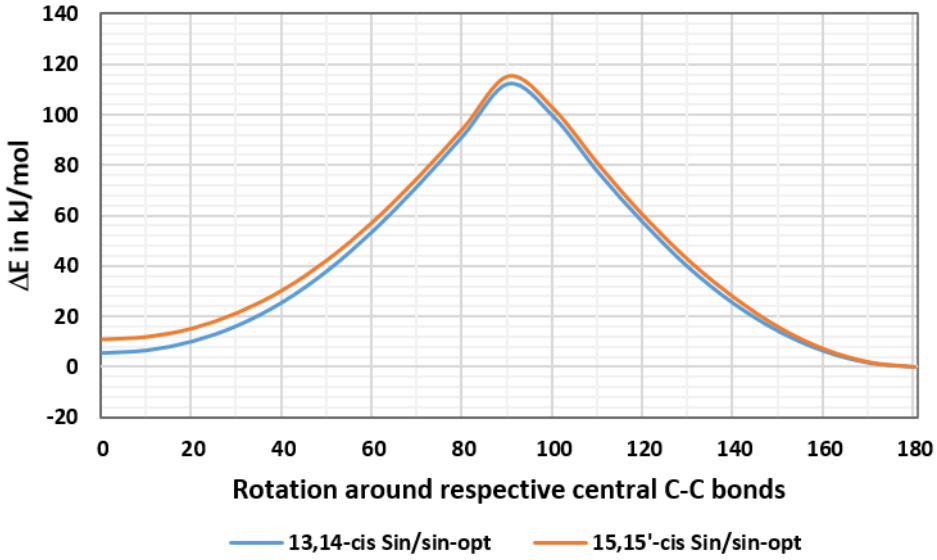

Figure S12. Variation in singlet state energy along C13-C14 (in 13,14-*cis*-) and C15-C15′ (in 15,15′-*cis*-spheroidene) bond rotations.

S8. Singlet-triplet crossing of the full 15,15′-*cis*-spheroidene along C14′-C13′ bond rotation

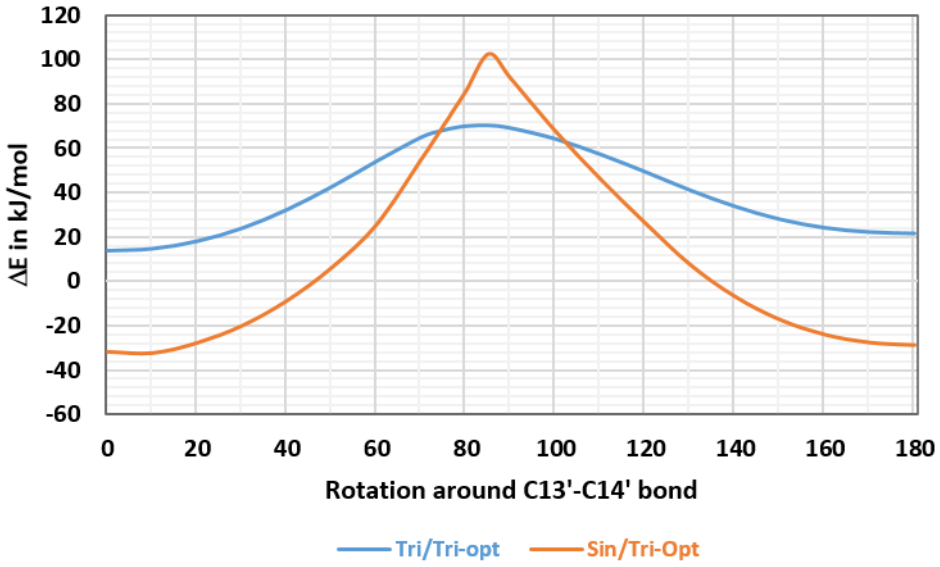

Figure S13. Singlet-triplet crossing of the full 15,15′-*cis*-spheroidene along C14′-C13′ bond rotation.

S9. Spheroidene (in light green) pigment's occupancy, in different angles, in the protein complex system. Structure (PDB id 2J8C) is taken from the ref 1.

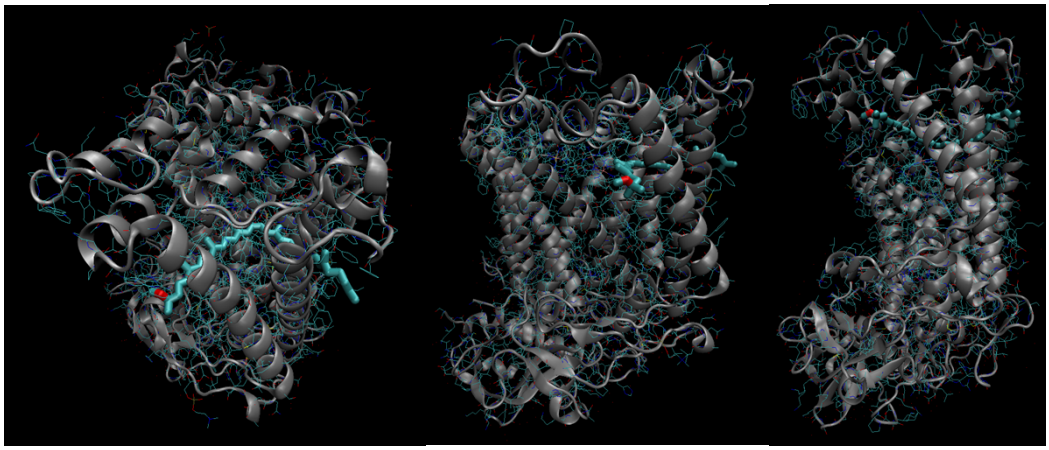

Figure S14. Spheroidene (in light green) pigment's occupancy, in different angles, in the protein complex system. Structure (PDB id 2J8C) is taken from the ref 1.

S10. Complete lists of the authors for references 58 and 59.

Reference 58

Gaussian 09, Revision B.01, M. J. Frisch, G. W. Trucks, H. B. Schlegel, G. E. Scuseria, M. A. Robb, J. R. Cheeseman, G. Scalmani, V. Barone, B. Mennucci, G. A. Petersson, H. Nakatsuji, M. Caricato, X. Li, H. P. Hratchian, A. F. Izmaylov, J. Bloino, G. Zheng, J. L. Sonnenberg, M. Hada, M. Ehara, K. Toyota, R. Fukuda, J. Hasegawa, M. Ishida, T. Nakajima, Y. Honda, O. Kitao, H. Nakai, T. Vreven, J. A. Montgomery, Jr., J. E. Peralta, F. Ogliaro, M. Bearpark, J. J. Heyd, E. Brothers, K. N. Kudin, V. N. Staroverov, R. Kobayashi, J. Normand, K. Raghavachari, A. Rendell, J. C. Burant, S. S. Iyengar, J. Tomasi, M. Cossi, N. Rega, J. M. Millam, M. Klene, J. E. Knox, J. B. Cross, V. Bakken, C. Adamo, J. Jaramillo, R. Gomperts, R. E. Stratmann, O. Yazyev, A. J. Austin, R. Cammi, C. Pomelli, J. W. Ochterski, R. L. Martin, K. Morokuma, V. G. Zakrzewski, G. A. Voth, P. Salvador, J. J. Dannenberg, S. Dapprich, A. D. Daniels, Ö. Farkas, J. B. Foresman, J. V. Ortiz, J. Cioslowski, and D. J. Fox, Gaussian, Inc., Wallingford CT, 2010.

Reference 59

Gaussian 09, Revision D.01, M. J. Frisch, G. W. Trucks, H. B. Schlegel, G. E. Scuseria, M. A. Robb, J. R. Cheeseman, G. Scalmani, V. Barone, B. Mennucci, G. A. Petersson, H. Nakatsuji, M. Caricato, X. Li, H. P. Hratchian, A. F. Izmaylov, J. Bloino, G. Zheng, J. L. Sonnenberg, M. Hada, M. Ehara, K. Toyota, R. Fukuda, J. Hasegawa, M. Ishida, T. Nakajima, Y. Honda, O. Kitao, H. Nakai, T. Vreven, J. A. Montgomery, Jr., J. E. Peralta, F. Ogliaro, M. Bearpark, J. J. Heyd, E. Brothers, K. N. Kudin, V. N. Staroverov, R. Kobayashi, J. Normand, K. Raghavachari, A. Rendell, J. C. Burant, S. S. Iyengar, J. Tomasi, M. Cossi, N. Rega, J. M. Millam, M. Klene, J. E. Knox, J. B. Cross, V. Bakken, C. Adamo, J. Jaramillo, R. Gomperts, R. E. Stratmann, O. Yazyev, A. J. Austin, R. Cammi, C. Pomelli, J. W. Ochterski, R. L. Martin, K. Morokuma, V. G. Zakrzewski, G. A. Voth, P. Salvador, J. J. Dannenberg, S. Dapprich, A. D. Daniels, Ö. Farkas, J. B. Foresman, J. V. Ortiz, J. Cioslowski, and D. J. Fox, Gaussian, Inc., Wallingford CT, 2013.

References

1. J. Koepke, E.-M. Krammer, A. R. Klingen, P. Sebban, G. M. Ullmann and G. Fritzsch, *Journal of Molecular Biology*, 2007, **371**, 396-409.
2. R. J. Cogdell and H. A. Frank, *Biochimica Et Biophysica Acta*, 1987, **895**, 63-79.
3. H. A. Frank and R. J. Cogdell, in *Carotenoids in Photosynthesis*, eds. A. Young and G. Britton, Chapman & Hall, London, 1993, pp. 252-326.
4. Y. Koyama, *Journal of Photochemistry and Photobiology B-Biology*, 1991, **9**, 265-280.
5. H. A. Frank and R. J. Cogdell, *Photochemistry and Photobiology*, 1996, **63**, 257-264.
6. G. Britton, S. Liaaen-Jensen and H. Pfander, *Carotenoids: Natural functions*, Birkhauser Verlag, Basel, 2008.
7. S. Lin, E. Katilius, A. K. W. Taguchi and N. W. Woodbury, *Journal of Physical Chemistry B*, 2003, **107**, 14103-14108.
8. S. Lin, E. Katilius, R. P. Ilagan, G. N. Gibson, H. A. Frank and N. W. Woodbury, *Journal of Physical Chemistry B*, 2006, **110**, 15556-15563.
9. T. Ritz, A. Damjanovic, K. Schulten, J. P. Zhang and Y. Koyama, *Photosynthesis Research*, 2000, **66**, 125-144.
10. A. Damjanovic, T. Ritz and K. Schulten, *Biophysical Journal*, 1998, **74**, A76-A76.
11. A. Damjanovic, T. Ritz and K. Schulten, *Physical Review E*, 1999, **59**, 3293-3311.
12. A. Damjanovic, T. Ritz and K. Schulten, *Biophysical Journal*, 1999, **76**, A239-A239.
13. A. Telfer, S. Dhami, S. M. Bishop, D. Phillips and J. Barber, *Biochemistry*, 1994, **33**, 14469-14474.
14. C. S. Foote, in *Free radicals in Biology*, ed. W. A. Pryor, Academic Press, New York, 1976, vol. II.
15. J. T. Landrum and R. A. Bone, *Archives of Biochemistry and Biophysics*, 2001, **385**, 28-40.
16. H. Nishino, *Journal of Cellular Biochemistry*, 1997, 86-91.
17. J. Lee, N. Koo and D. B. Min, *Comprehensive Reviews in Food Science and Food Safety*, 2004, **3**, 21-33.
18. A. deWinter and S. G. Boxer, *Journal of Physical Chemistry B*, 1999, **103**, 8786-8789.
19. H. A. Frank, in *The photosynthetic reaction center*, eds. J. R. Norris and J. Deisenhofer, Academic Press, New York, 1993, vol. 2, ch. 9, pp. 221-237.
20. Y. Koyama and H. Hashimoto, in *Carotenoids in photosynthesis* eds. A. Young and G. Britton, Chapmann & Hall, London, 1993, pp. 327-409.
21. Y. Koyama, M. Kuki, P. O. Andersson and T. Gillbro, *Photochemistry and Photobiology*, 1996, **63**, 243-256.
22. A. Telfer, *Philosophical Transactions of the Royal Society of London Series B-Biological Sciences*, 2002, **357**, 1431-1439.
23. R. J. Cogdell, T. D. Howard, R. Bittl, E. Schlodder, I. Geisenheimer and W. Lubitz, *Philosophical Transactions of the Royal Society of London Series B-Biological Sciences*, 2000, **355**, 1345-1349.
24. P. Horton, A. V. Ruban and A. J. Young, *Photochemistry of Carotenoids*, 1999, **8**, 271-291.
25. K. K. Niyogi, O. Bjorkman and A. R. Grossman, *Proceedings of the National Academy of Sciences of the United States of America*, 1997, **94**, 14162-14167.
26. A. V. Ruban, R. Berera, C. Ilioaia, I. H. M. van Stokkum, J. T. M. Kennis, A. A. Pascal, H. van Amerongen, B. Robert, P. Horton and R. van Grondelle, *Nature*, 2007, **450**, 575-U522.
27. S. Santabarbara and D. Carbonera, *The Journal of Physical Chemistry B*, 2005, **109**, 986-991.
28. F. Boucher and G. Gingras, *Photochemistry and Photobiology*, 1984, **40**, 277-281.
29. M. Kuki, M. Naruse, T. Kakuno and Y. Koyama, *Photochemistry and Photobiology*, 1995, **62**, 502-508.

30. H. Hashimoto and Y. Koyama, *Journal of Physical Chemistry*, 1988, **92**, 2101-2108.
31. H. Hashimoto, Y. Koyama, K. Ichimura and T. Kobayashi, *Chemical Physics Letters*, 1989, **162**, 517-522.
32. M. Kuki, Y. Koyama and H. Nagae, *Journal of Physical Chemistry*, 1991, **95**, 7171-7180.
33. Y. Koyama, Y. Mukai and M. Kuki, *SPIE (Laser Spectroscopy of Bio-molecules)*, 1993, **1921**, 191-202.
34. N. Ohashi, N. KoChi, M. Kuki, T. Shimamura, R. J. Cogdell and Y. Koyama, *Biospectroscopy*, 1996, **2**, 59-69.
35. J. A. Bautista, V. Chynwat, A. Cua, F. J. Jansen, J. Lugtenburg, D. Gosztola, M. R. Wasielewski and H. A. Frank, *Photosynthesis Research*, 1998, **55**, 49-65.
36. R. Fujii, K. Furuichi, J. P. Zhang, H. Nagae, H. Hashimoto and Y. Koyama, *Journal of Physical Chemistry A*, 2002, **106**, 2410-2421.
37. Y. Mukai-Kuroda, R. Fujii, N. Ko-chi, T. Sashima and Y. Koyama, *Journal of Physical Chemistry A*, 2002, **106**, 3566-3579.
38. Z. D. Pendon, J. O. Sullivan, I. van der Hoef, J. Lugtenburg, A. Cua, D. F. Bocian, R. R. Birge and H. A. Frank, *Photosynthesis Research*, 2005, **86**, 5-24.
39. Z. D. Pendon, G. N. Gibson, I. van der Hoef, J. Lugtenburg and H. A. Frank, *Journal of Physical Chemistry B*, 2005, **109**, 21172-21179.
40. Z. D. Pendon, I. der Hoef, J. Lugtenburg and H. A. Frank, *Photosynthesis Research*, 2006, **88**, 51-61.
41. A. W. Roszak, K. McKendrick, A. T. Gardiner, I. A. Mitchell, N. W. Isaacs, R. J. Cogdell, H. Hashimoto and H. A. Frank, *Structure*, 2004, **12**, 765-773.
42. Y. Kakitani, R. Fujii, Y. Koyama, H. Nagae, L. Walker, B. Salter and A. Angerhofer, *Biochemistry*, 2006, **45**, 2053-2062.
43. A. C. Wirtz, M. C. van Hemert, J. Lugtenburg, H. A. Frank and E. J. J. Groenen, *Biophysical Journal*, 2007, **93**, 981-991.
44. G. Mathies, M. C. van Hemert, P. Gast, K. B. S. S. Gupta, H. A. Frank, J. Lugtenburg and E. J. J. Groenen, *Journal of Physical Chemistry A*, 2011, **115**, 9552-9556.
45. J. M. Boereboom, M. C. van Hemert and J. Neugebauer, *Chemphyschem*, 2011, **12**, 3157-3169.
46. K. Schulten and M. Karplus, *Chemical Physics Letters*, 1972, **14**, 305-&.
47. K. Schulten, I. Ohmine and M. Karplus, *Journal of Chemical Physics*, 1976, **64**, 4422-4441.
48. D. Ghosh, J. Hachmann, T. Yanai and G. K. L. Chan, *Journal of Chemical Physics*, 2008, **128**.
49. C. M. Marian, S. C. Kock, C. Hundsdorfer, H. D. Martin, W. Stahl, E. Ostroumov, M. G. Muller and A. R. Holzwarth, *Photoch Photobio Sci*, 2009, **8**, 270-278.
50. E. Ostroumov, M. G. Muller, C. M. Marian, M. Kleinschmidt and A. R. Holzwarth, *Phys Rev Lett*, 2009, **103**.
51. M. Kleinschmidt, C. M. Marian, M. Waletzke and S. Grimme, *Journal of Chemical Physics*, 2009, **130**.
52. J. P. Ceron-Carrasco, A. Requena and C. M. Marian, *Chemical Physics*, 2010, **373**, 98-103.
53. M. Macernis, J. Sulskus, C. D. P. Duffy, A. V. Ruban and L. Valkunas, *Journal of Physical Chemistry A*, 2012, **116**, 9843-9853.
54. S. Knecht, C. M. Marian, J. Kongsted and B. Mennucci, *Journal of Physical Chemistry B*, 2013, **117**, 13808-13815.
55. J. P. Gotze, D. Kroner, S. Banerjee, B. Karasulu and W. Thiel, *Chemphyschem*, 2014, **15**, 3391-3400.
56. O. Andreussi, S. Knecht, C. M. Marian, J. Kongsted and B. Mennucci, *J Chem Theory Comput*, 2015, **11**, 655-666.
57. A. D. Becke, *Physical Review A*, 1988, **38**, 3098-3100.
58. C. T. Lee, W. T. Yang and R. G. Parr, *Physical Review B*, 1988, **37**, 785-789.
59. J. P. Perdew, *Physical Review B*, 1986, **33**, 8822-8824.

60. *Journal*.
61. Y. Zhao and D. G. Truhlar, *Theoretical Chemistry Accounts*, 2008, **120**, 215-241.
62. R. Peverati and D. G. Truhlar, *Journal of Physical Chemistry Letters*, 2011, **2**, 2810-2817.
63. T. Schwabe and S. Grimme, *Physical Chemistry Chemical Physics*, 2007, **9**, 3397-3406.
64. C. Moller and M. S. Plesset, *Physical Review*, 1934, **46**, 0618-0622.
65. M. Head-Gordon, J. A. Pople and M. J. Frisch, *Chemical Physics Letters*, 1988, **153**, 503-506.
66. G. D. Purvis and R. J. Bartlett, *Journal of Chemical Physics*, 1982, **76**, 1910-1918.
67. G. E. Scuseria, C. L. Janssen and H. F. Schaefer, *Journal of Chemical Physics*, 1988, **89**, 7382-7387.
68. J. A. Pople, M. Head-Gordon and K. Raghavachari, *Journal of Chemical Physics*, 1987, **87**, 5968-5975.
69. C. E. Dykstra, *Chemical Physics Letters*, 1977, **45**, 466-469.
70. N. C. Handy, J. A. Pople, M. Head-Gordon, K. Raghavachari and G. W. Trucks, *Chemical Physics Letters*, 1989, **164**, 185-192.
71. R. Kobayashi, N. C. Handy, R. D. Amos, G. W. Trucks, M. J. Frisch and J. A. Pople, *Journal of Chemical Physics*, 1991, **95**, 6723-6733.
72. T. H. Dunning, *Journal of Chemical Physics*, 1989, **90**, 1007-1023.
73. E. F. C. Byrd, C. D. Sherrill and M. Head-Gordon, *Journal of Physical Chemistry A*, 2001, **105**, 9736-9747.
74. G. J. O. Beran, S. R. Gwaltney and M. Head-Gordon, *Physical Chemistry Chemical Physics*, 2003, **5**, 2488-2493.
75. C. J. Cramer, *Essentials of computational chemistry*, John Wiley & Sons, Ltd, England, 2002.